

## Applications of Fast Response Continuous SF<sub>6</sub> Analyzers to In Situ Cloud Studies

JEFFREY L. STITH

*University of North Dakota, Grand Forks, ND 58202*

RICHARD L. BENNER

*North American Weather Consultants, Salt Lake City, UT 84117*

(Manuscript received 3 October 1986, in final form 26 March 1987)

### ABSTRACT

The airborne applications of two recently developed analyzers for sulfur hexafluoride (SF<sub>6</sub>) to investigations of cloud top mixing and cloud seeding are described. The analyzers were developed by AeroVironment (AV) and by Washington State University (WSU). Both analyzers were capable of detecting cumulus-scale plume features. The more elaborate flow control mechanism in the AV analyzer was helpful in reducing the effects of altitude on the instrument response, while the faster response and lower baseline noise level of the WSU analyzer were necessary to detect many plume features.

A midcloud injection of SF<sub>6</sub> was followed as it mixed through the tops of a small cumulus cloud. The tracer plume was first detected upshear, then mixed through the cloud top region as the cloud top began to collapse.

A plume of AgI cloud seeding agent mixed with SF<sub>6</sub> was used to investigate the activation and growth of ice particles in a stratocumulus cloud which was overseeded. The SF<sub>6</sub> tracer and ice particle plumes remained colocated during the 45 min sampling period, except for one region of ice particles which had begun to separate from the SF<sub>6</sub> 26 min after the cloud was treated. The growth of ice was limited by water vapor diffusion into the seeding plume. The measured tracer concentrations were used to estimate the fraction of the seeding nuclei which had activated and grown to detectable sizes. A maximum fraction of 54% was observed 17.5 min after seeding.

Several other applications for SF<sub>6</sub> tracer applications are recommended.

### 1. Introduction

The recent development of fast response analyzers for sulfur hexafluoride (SF<sub>6</sub>) has made it possible to sample small atmospheric plumes of SF<sub>6</sub> in real time with research aircraft. This allows SF<sub>6</sub> to be used as a tracer in studies of relatively small-scale (<1 km) atmospheric features, such as individual cumulus cloud elements. For example, by injecting the tracer into a cloud and then following the history of the tracer plume, it should be possible to follow subsequent mixing of the plume in the cloud and the exchange of air between cloud and environmental air (i.e., entrainment and detrainment). Most previous studies of cloud mixing relied on thermodynamic analyses to infer the history of the mixing process in cumulus clouds. In this paper we describe the application of two recently developed fast response SF<sub>6</sub> analyzers to studies of plume mixing and ice activation in clouds.

The studies are part of the NOAA Federal State Cooperative Program (Reinking, 1985) to evaluate the North Dakota state cloud seeding program. Our studies address two long-standing questions in cloud seeding: first, when a cloud is treated, does enough of the seeding agent reliably mix through the proper regions of the clouds for the agent to properly affect the cloud; and second, does the agent actually produce the expected

amounts of ice, based on laboratory-derived effectiveness of the seeding agent? To function properly, the tracer must be insoluble in water and must diffuse with the plume of artificial ice nuclei and ice particles. For SF<sub>6</sub>, the first condition is easily satisfied, because SF<sub>6</sub> is essentially insoluble in water. The second is satisfied for at least the first 10 min of ice crystal growth, which is long enough for the ice crystals to grow to easily detectable sizes (see Stith et al., 1986).

Because direct measurements of ice nuclei concentrations are difficult, at best, studies of the effects of glaciogenic cloud seeding agents, such as silver iodide (AgI) smokes, often rely on measurements of the plume of ice particles produced by the agent (e.g., Marwitz and Stewart, 1981). Measuring these "seeding signatures" is important because the amount of ice produced and the rate of ice production has been found in laboratory studies (e.g., DeMott et al., 1983) to be a strong function of the type of AgI smoke used (i.e., AgI smokes produced by burning various mixtures in flares or in acetone AgI burners).

The formation of ice in atmospheric clouds by AgI smokes is also influenced by the irregular environment within the cloud. For example, variations in supersaturation, droplet concentration, temperature, vertical wind, and turbulence may all affect the concentration of ice particles in the cloudy AgI plume, which is a

function of time even in steady conditions. The concentration of ice in supercooled plumes of AgI increases with the downwind travel time, but exhibits large fluctuations (e.g., Marwitz and Stewart, 1981). These fluctuations may result from fluctuations in the concentrations of AgI smoke due to the turbulent diffusion in the plume, or uneven activation and growth of the AgI ice nuclei within the plume. By releasing SF<sub>6</sub> along with the AgI smoke, the effects of diffusion can be accounted for, allowing the activation process to be studied separately. This technique is described in section 3.

In the Stith et al. paper, a summary of the general characteristics of plumes of SF<sub>6</sub> and seeding agents in a variety of cumulus clouds is given. The materials were injected into the bases or midlevels of summertime clouds near Dickinson, ND, during 1984 and 1985. Plumes sampled at midlevels were found to be relatively narrow and embedded within updrafts or downdrafts; relatively high concentrations of the tracer were observed in some downdrafts. Plumes with diameters comparable to the cloud diameters were found in the upper portions of the clouds. In the present paper we examine the performance of the two analyzers used in that study and elaborate on two cases from 1985. The first case illustrates an application of these analyzers and SF<sub>6</sub> in studying cloud-top mixing. The second demonstrates the use of the SF<sub>6</sub> tracer technique in the interpretation of seeding signatures.

## 2. Instrumentation

Two continuous analyzers were used for simultaneous detection of the SF<sub>6</sub> plumes. Both analyzers rely on electron capture detectors (Simmonds et al., 1976), but operate the detectors in a different manner, as discussed below. The two analyzers also differ in their temperature, pneumatic configuration, pressure, and gas control mechanisms. The first analyzer, built by AeroVironment Inc. (AV), incorporates electronic mass flow controllers for rigorous control of the sample air, hydrogen flow rates, and the absolute pressure of the analyzer flow system. The electron capture detector is operated in a constant current mode, which requires a change in the standing current of the detector to adjust the signal baseline. This change also affects the response to SF<sub>6</sub> and therefore the calibration curve. The second analyzer, built at Washington State University (WSU), was designed specifically to achieve the fastest response possible and to reduce power consumption to a minimum. The WSU analyzer uses a constant pulse mode of operation of the electron capture detector. In this mode a change in the signal baseline is purely an electronic offset which does not affect the response to SF<sub>6</sub>. A detailed discussion of both specific instrument designs can be found in Baxter et al. (1983) and Benner and Lamb (1985), for the AV and WSU analyzers, respectively.

Cloud and SF<sub>6</sub> measurements were obtained from the University of North Dakota Cessna Citation re-

search aircraft. In addition to the SF<sub>6</sub> analyzers, it carried Particle Measuring Systems (PMS) probes for measuring cloud and precipitation size spectra, an Inertial Navigation/Gust Probe system for wind and turbulence measurements, a Johnson-Williams (JW) hot-wire cloud liquid water sensor, a NCAR type reverse-flow temperature sensor, a dewpoint hygrometer (Cambridge System design), and pressure transducers for measuring static and pitot pressures. A PMS two-dimensional imaging probe (model 2D-C) with pixel resolution of 35  $\mu\text{m}$  was used for measurement of ice particle concentrations. All measurements were digitally recorded by the Citation data system and displayed in real time aboard the aircraft. Data processing followed relatively standard procedures, as in Veal et al. (1977) for standard aircraft meteorological parameters and MacCready (1964) for computation of the turbulent energy dissipation rate,  $\epsilon$ .

A separate seeder aircraft was used to dispense SF<sub>6</sub> of 99.5% purity through a flow control system which exhausted near both wingtips. Silver iodide seeding aerosols were dispersed by wingtip acetone burners. For this study an AgI-AgCl aerosol was produced. The laboratory-derived nucleation characteristics of this aerosol are described in DeMott et al., (1983). More details on the aircraft system and treatment procedures for both of the aircraft are in Stith et al., (1986).

Both analyzers were routinely calibrated with premixed SF<sub>6</sub> standard gases (Scott-Marrin Inc., Riverside, CA). The voltage output (response) to a 3530 ppt standard gas varied over the one-month field program by a maximum of 18.3 and 3.7% for the AV and WSU analyzers, respectively, during ground testing. The different modes of detector operation in the two instruments were responsible for the marked differences in the day-to-day variation in the responses of the two instruments. This does not, however, reflect the consistency of the responses on any single day. Both analyzers displayed very good response stability over any single day (i.e., <2% change). The WSU analyzer displayed a linear response to the calibration gas, while the AV was essentially linear below 1000 ppt and somewhat nonlinear at the higher concentrations (Fig. 1). Since the SF<sub>6</sub> concentrations observed in our field studies were less than 1000 ppt, linear regressions were used to convert the voltage responses to equivalent ppt SF<sub>6</sub>.

Test flights early in the field program revealed that the small sample pump used in the WSU analyzer was unable to maintain sample flow above about 4.6 km (MSL, pressure altitude). Sample flow was adequately maintained by the AV analyzer to 8.5 km MSL. To overcome the problem with the WSU instrument, a dual-stage pump was placed upstream of the WSU analyzer which delivered 5 l min<sup>-1</sup> of outside air to a tee with one end open to the aircraft cabin and the other end connected to the WSU analyzer inlet. The inlet required a sample flow of only about 0.07 l min<sup>-1</sup>. This procedure allowed the WSU analyzer to operate at es-

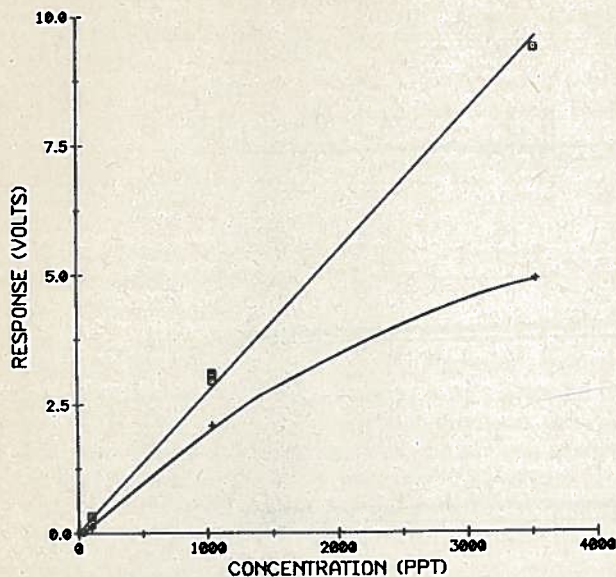


FIG. 1. Calibration curves, based on the voltage response to  $\text{SF}_6$  standard gases, for the AV (crosses) and WSU (boxes) analyzers.

entially cabin pressure and to operate at all sampling altitudes used in the study (up to 8.5 km). This procedure also decreased the baseline drift of the instrument associated with altitude changes, because cabin pressure fluctuations are normally much less than ambient fluctuations.

The baseline drifts caused by changes in altitude were different for each instrument. The AV analyzer would drift with rapid changes in elevation but would come back to nearly the previous baseline after the mass flow controllers had acclimated to the new pressure level. The WSU analyzer would drift with cabin pressure rather than ambient pressure. For the Citation the cabin pressure was maintained at about 2 km, equivalent pressure altitude, at typical sampling altitudes of 5 km; however, it would fluctuate slightly as power changes were made. This caused small ( $\sim 15$ – $20$  ppt) peaks to occur on the WSU instrument when power was cut drastically and reapplied. Once this problem was identified it was minimized by carefully controlling the aircraft cabin pressure during sampling runs. Maximum rate of baseline drift occurred during landing and take-off where both instruments could drift as much as 100 ppt per minute. During operational sampling neither instrument exceeded a drift rate of 20 ppt/min. This value is greater than previously reported for either instrument and is probably due to sampling while performing the rapid maneuvers that were required for collecting repeated samples of plumes in convective clouds.

A pressure effect was noted in the response of the two instruments. This was determined by injecting a standard gas into the sample manifold at ambient pressure at various altitudes from 0.9 to 6.4 km. The results are presented in Fig. 2. The AV response de-

creased about 0.25% per 100 m and the WSU response decreased about 0.42% per 100 m. The decrease in the instruments' response with altitude was somewhat unexpected, since both instruments operate with mass flow control. However, the difference between the two instruments is undoubtedly due to the fact that the AV analyzer controls the absolute pressure of the sample gas but the WSU analyzer does not. The pressure effect will reduce the observed concentrations at typical sampling altitudes (5 km) by about 12% and 21% for the AV and WSU analyzers, respectively.

Baseline noise levels for both instruments were also measured during the field program. Ground testing indicated a (peak-to-peak) noise level of about 30 ppt (0.04 V) and 5 ppt (0.015 V) for the AV and WSU analyzers, respectively. These values are slightly higher than previously reported, and possibly reflect different operating conditions in the field. In the aircraft the WSU baseline noise level was about 9 ppt (0.028 V) and steady. The baseline noise of the AV varied somewhat with ambient conditions from 30 to 60 ppt (0.04 to 0.05 V). During flight, voltage spikes of up to 0.04 V were recorded on the channels for both instruments due to electrical interference in the cabin. These spikes were of very short duration and only affected one high-frequency sample (at 24 hertz sampling rate); consequently, they did not interfere with plume detection.

Measurements in an untreated cumulus cloud (Fig. 3) revealed that the WSU baseline noise was not affected by the cloud or turbulent conditions in the cloud. The AV analyzer noise increased from 30 to about 60 ppt (0.04 to 0.05 V) during passage through turbulent conditions (Fig. 3), probably due to rapid accelerations which might have affected the flow control system.

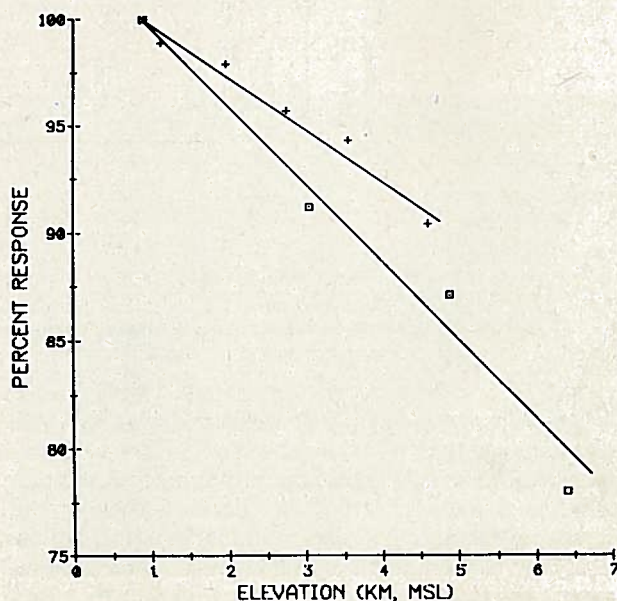


FIG. 2. The change in instrument response with elevation (pressure altitude) for the AV (crosses) and WSU (boxes) analyzers.

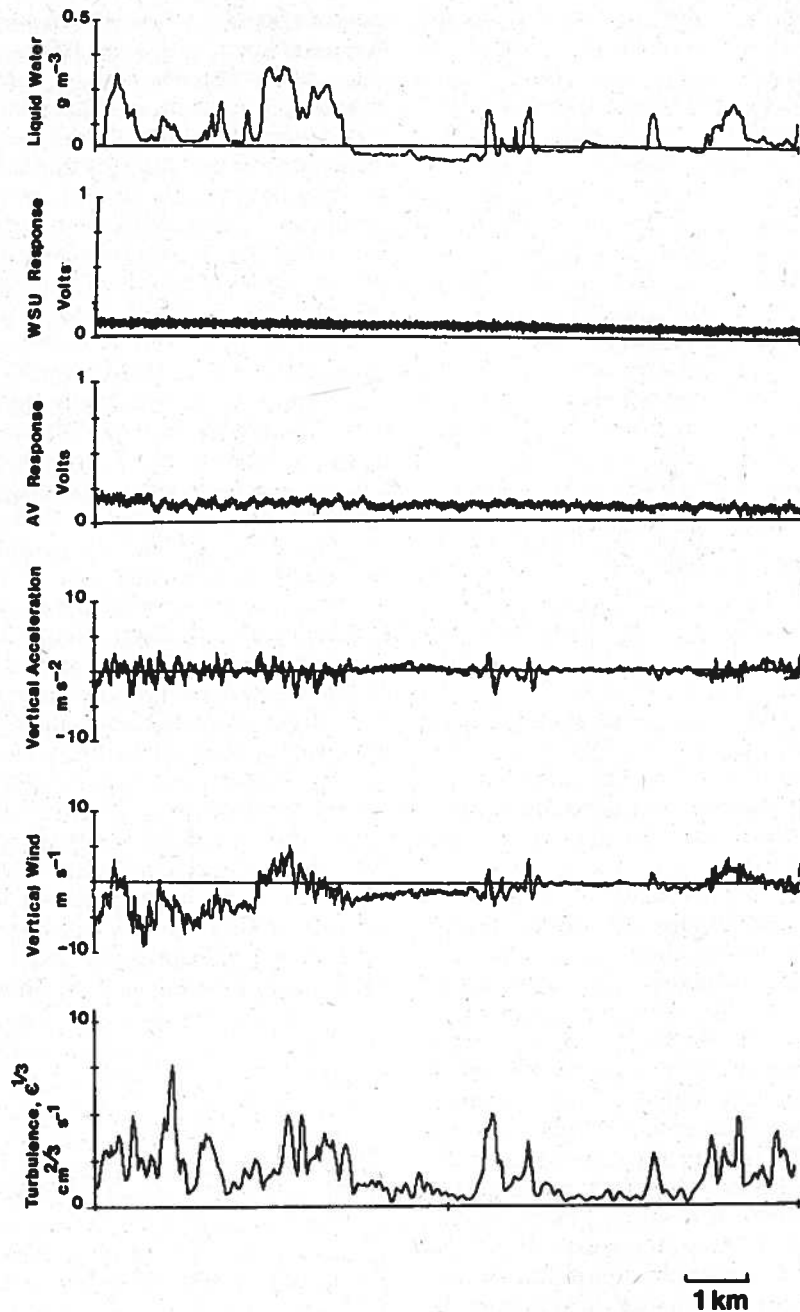


FIG. 3. Voltage response of the AV and WSU analyzers during sampling in an untreated cumulus cloud at 5.5 km (MSL) altitude. Also shown are the cloud liquid water concentrations, the vertical accelerations of the aircraft, vertical wind, and turbulence.

Response and lag times measured during the field program are shown in Table 1. These tests were performed with an instantaneous injection of  $\text{SF}_6$  calibration gas at the junction of the sample inlet tube and the aircraft manifold to determine the responses of the analyzers as configured on the Citation. Measured response times for both analyzers were slower than previously reported values, due to longitudinal mixing of the injected gas within the 1 m of 0.5 cm (internal

diameter) sample tubing, which was upstream of the analyzers. Since the volume of the sample inlet tube was only about  $20 \text{ cm}^3$ , and the flowrate drawn by both analyzers was about  $10 \text{ l min}^{-1}$ , the sample tube accounts for only  $0.12 \text{ s}$  ( $<5\%$ ) of the measured lag times. The differences in response times of the two instruments were quite apparent during sampling (Fig. 4). During 1985 much of the  $\text{SF}_6$  sampling was done in relatively small dilute plumes which were detected most

TABLE 1. Lag and response times in the aircraft configuration.

Lag times (s)		% of signal deflection	Average response times (s)		
AV	WSU		AV	WSU without upstream pump	WSU with upstream pump
3.7 ± 0.1	2.5 ± 0.2	0-63	1.65	0.53	0.85
		0-90	3.50		1.85
		5-95	4.75	0.90	2.30

easily by the WSU analyzer, due to its faster response and lower noise levels. Of 117 SF<sub>6</sub> plumes detected by the WSU analyzer, only 28 were evident on the AV analyzer. Many dilute plumes may have been missed by both instruments. A relatively low SF<sub>6</sub> release rate was used for these studies (0.02 to 0.07 kg km<sup>-1</sup>). Higher release rates are planned in the future to improve plume detection.

### 3. Applications

#### a. Mixing and dispersion of a SF<sub>6</sub> plume in the top of a cumulus cloud

On 19 July 1985, a small cumulus cloud (Fig. 5) was treated with 0.016 kg km<sup>-1</sup> of SF<sub>6</sub> and the AgI-

AgCl seeding agent by a single treatment pass at 4270 m at 1923 MDT. The height of the cloud top was approximately 4820 m, based upon an aircraft pass through the top at 1928:30 MDT. Cloud-top temperature was only -6°C, which evidently did not activate the seeding agent, as no ice was found. Cloud bases in the area were observed earlier (at 1800 MDT) to be 3350 m. An ambient sounding made while descending from the area at 1945 to 1955 is presented in Fig. 6. The sounding revealed an almost adiabatic region of uniform mixing ratio at low levels (910 to 760 mb) and a dry slightly stable upper region between 520 and 640 mb. A sharp transition between the dry upper level and a moist region below 640 mb was observed; however, the dewpoint hygrometer was unable to heat fast enough to properly measure the ambient dewpoints in the intermediate level during the descent of the Citation. The lifting condensation level of the lower-level air was about 700 mb (or 3 km pressure altitude). During the sounding the average wind at cloud top (550 mb) was 300° at 16 m s<sup>-1</sup>, at cloud midlevels (600 mb) the wind was 302° at 12 m s<sup>-1</sup>, and near cloud base (700 mb) the wind was 252° at 6 m s<sup>-1</sup>. In the sampling region near cloud tops at 550-600 mb the vertical wind shear was primarily speed shear; between cloud base

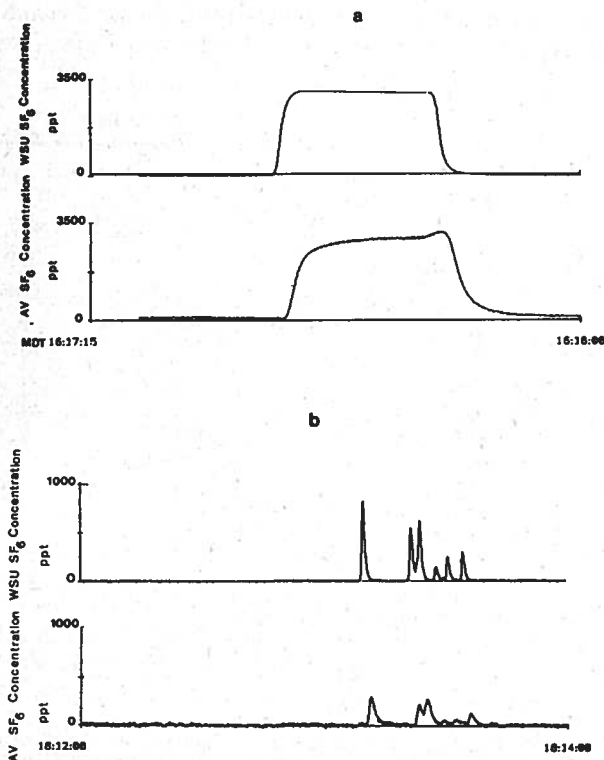


FIG. 4. The response of the AV and WSU analyzers to (a) a test pulse of 3350 ppt calibration gas during flight at 5.5 km (MSL) and (b) to a plume of SF<sub>6</sub>, sampled about 2 km behind the release aircraft at an altitude of 2.7 km.



FIG. 5. The cumulus cloud region just prior to treatment at 1919 MDT 19 July 1985. The photo is looking north, with the treated cloud region in the upper left-hand portion of the photograph.

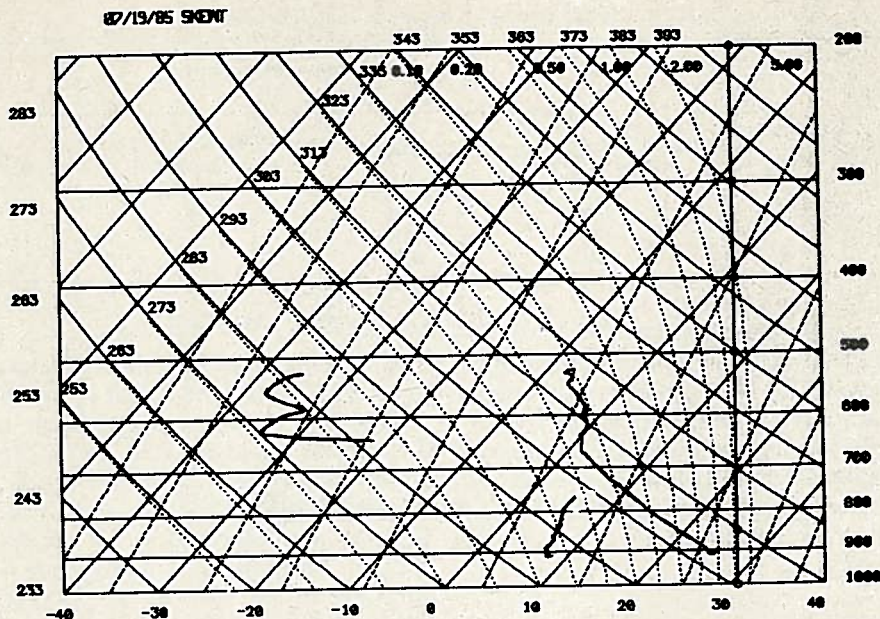


FIG. 6. The result of a partial sounding made on descent from the cloud sampling region, 1942 to 1954 MDT 19 July 1985. A portion of the dewpoint data is unreliable between 640 and 760 mb; see text for explanation.

and cloud top the upshear region was to the northwest.

Seven passes through a single cloud turret were made. The flight path of the Citation, relative to the cloud at 570 mb is presented in Fig. 7. The results of the measurements are presented in Figs. 8 and 9. Pass 1 (see Figs. 7 and 8) was made during treatment, 270 m above the treatment aircraft at 4540 m, on a northwestern track parallel to the treatment aircraft. The main liquid water region at the time of treatment was in updraft. Downwind (also downshear) the air was considerably more turbulent than upwind. The cloud and downwind regions were colder than the ambient air upwind, suggesting that although the cloud was ascending at this point, it had negative buoyancy. Pass number 2, which was made at the same altitude in a southeasterly direction, revealed similar features (Fig. 8), except that the updraft had decreased considerably and the liquid water concentrations were lower, indicating that the cloud was evaporating and slowing its upward ascent during the 2-minute period between the measurements. The third pass was made in the visual tops of the cloud on a parallel track to pass 2 (Fig. 7) at 4820 m. This region was relatively calm and located on the edge of a  $7 \text{ m s}^{-1}$  downdraft (Fig. 8). The downdraft was just southeast of the liquid water region. On pass 4, made in a northwesterly direction at 4600 m, the plume of  $\text{SF}_6$  was observed in the northwestern portion of the cloud (Fig. 8). The southeastern portion of the cloud was starting to descend, while the northwest portion was still ascending slightly. The plume had ascended 330 m in 6.3 min. after treatment, for an average ascent rate prior to pass 4 of  $0.9 \text{ m s}^{-1}$ .

On pass 5, made in an easterly direction at 4600 m, the  $\text{SF}_6$  plume filled the entire liquid water and downdraft region. The downdraft had developed to over  $-5 \text{ m s}^{-1}$  on the eastern edge of the cloud, and liquid water content had decreased from that measured during pass

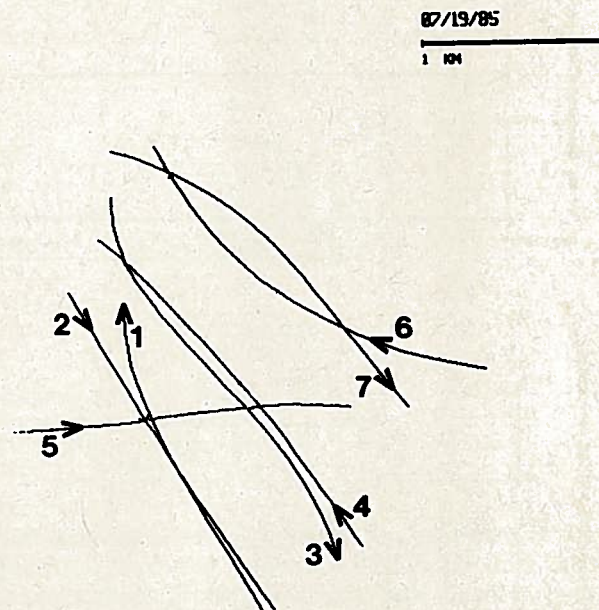


FIG. 7. Flight path of the Citation in a cloud-relative (Lagrangian) coordinate system, based on the sampling-level horizontal wind, for passes 1 through 7 on 19 July 1985. Passes 1, 2 and 7 were at an altitude of 4540 m (MSL), pass 3 at 4820 m, passes 4 and 5 at 4600 m, and pass 6 at 4650 m.

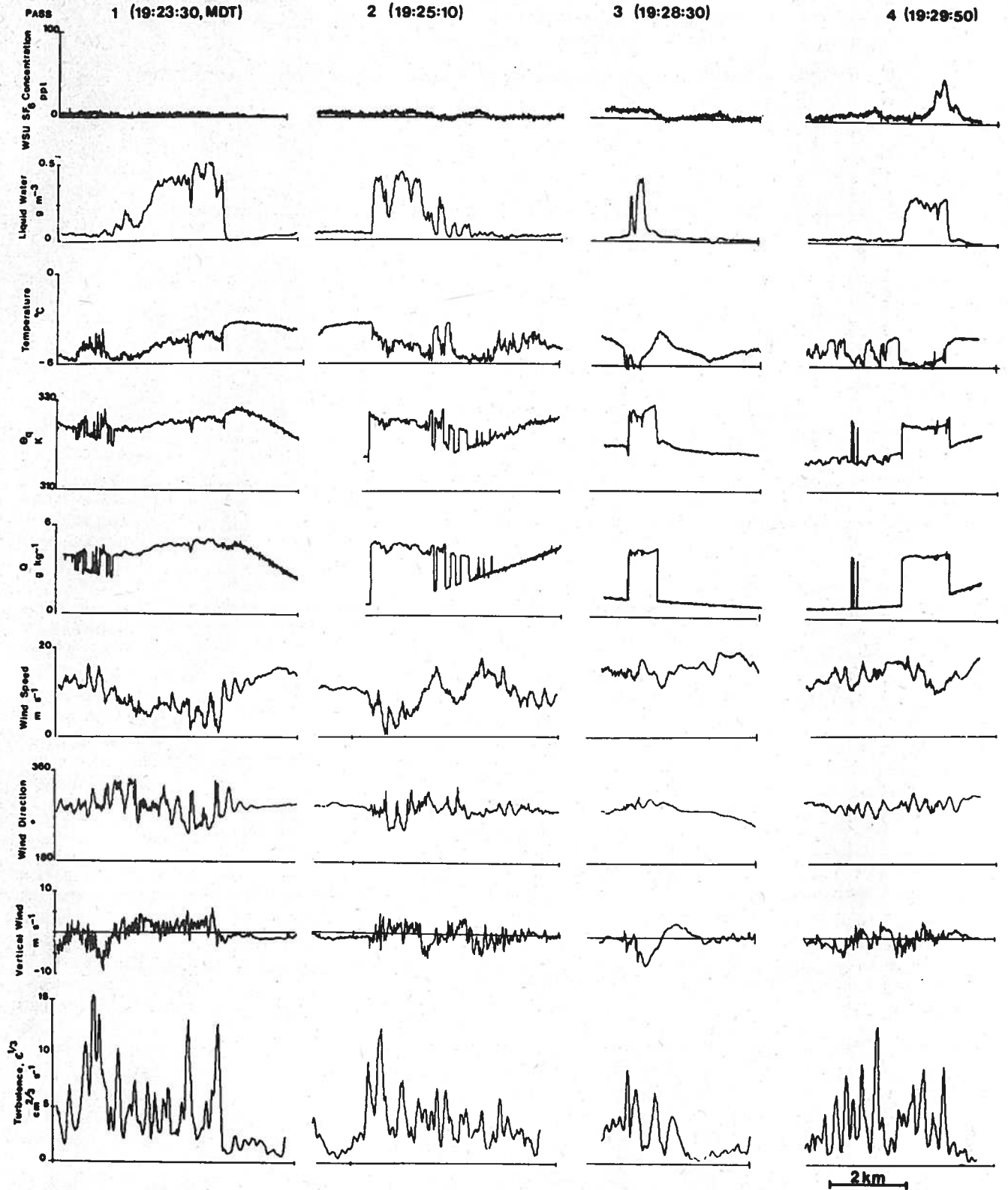


FIG. 8. The results of the measurements from passes 1 through 4 on 19 July 1985. The wet equivalent potential temperature  $\theta_w$ , and the total mixing ratio,  $Q$ , were computed in the cloud using the reverse-flow temperature measurements instead of those from the dew point hygrometer.

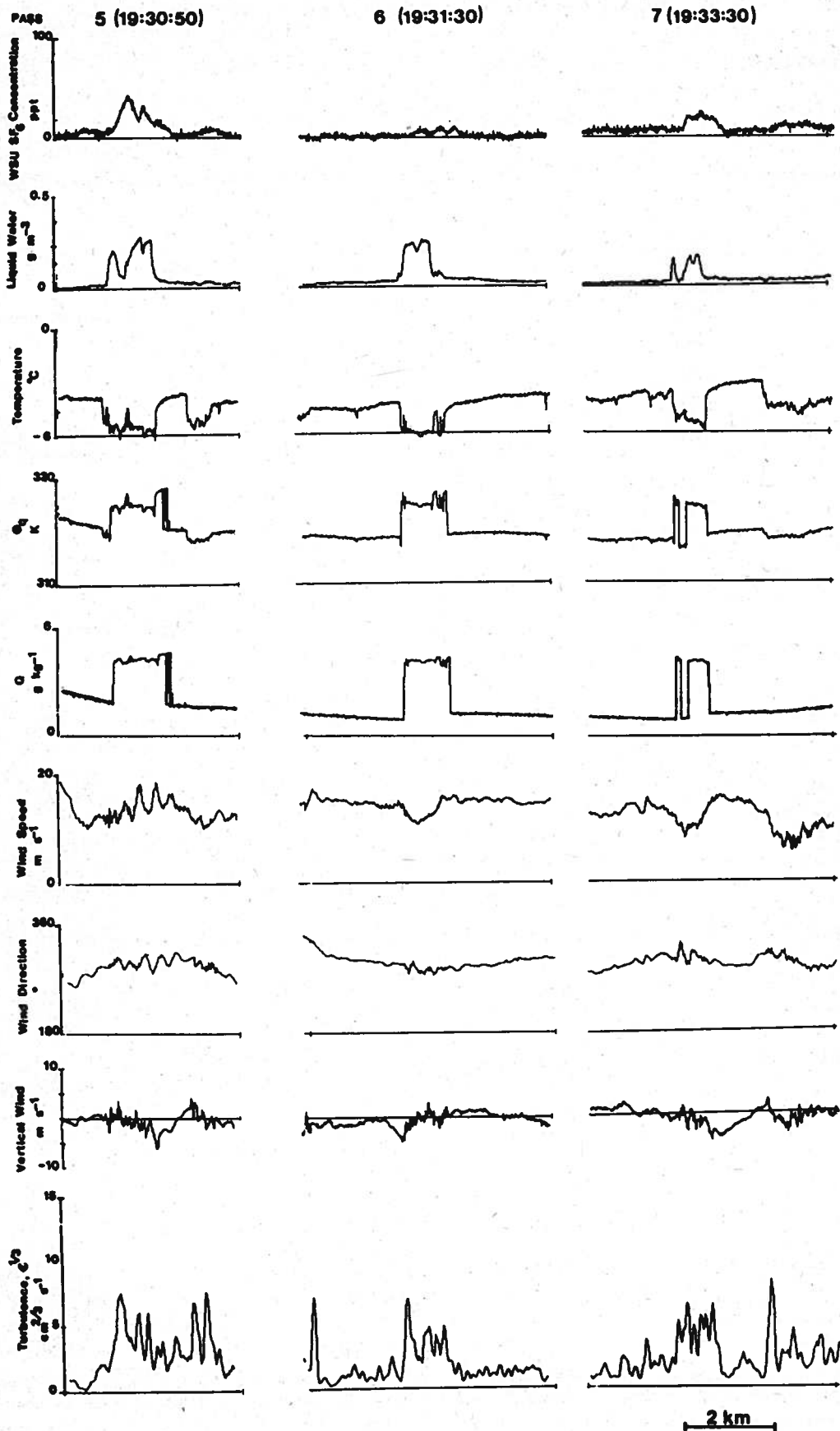


FIG. 9. As in Fig. 8 except for passes 5 through 7.

4. Pass 6, made in a northwesterly direction at 4650 m (about 500 m northeast of passes 1 through 5), missed most of the plume. However, the SF<sub>6</sub> plume was detected in that vicinity during pass 7 at a slightly lower altitude (4540 m).

At the beginning of the sampling the horizontal wind in the northwest portion of the cloud turret was similar to that near cloud base (e.g., Fig. 8, pass 1 and 2). During the later passes the horizontal wind throughout the turret gradually approached the value in the ambient air (Fig. 9). This suggests that during the time the plume was mixing through the cloud, the newer cloud regions were accelerating to the ambient horizontal wind.

Two conservative mixing parameters, the total water (liquid plus vapor) mixing ratio,  $Q$ , and the wet equivalent potential temperature  $\theta_q$  are also presented in Figs. 8 and 9. These were computed by assuming the air to be saturated in the cloud, using the reverse flow temperature sensor, since the hygrometer could not respond fast enough to measure the dew point in the clouds. Regions in the clouds which may have been undersaturated would have considerably lower values for these parameters than those computed. The  $Q$  and  $\theta_q$  in dry ambient air at 570 mb were about 1.5 g kg<sup>-1</sup> and 318 K, respectively. For pass 1 and 2, the in-cloud values were greatest in the northwest portion of the cloud. For the remainder of the passes these values were relatively constant across the cloud, indicating a well-mixed cloud; however, values near the center of the cloud were slightly less than those near the edge for passes 3 and 4 (Fig. 8). Values from pass 3, the highest pass, were comparable or slightly higher than in the cloud below.

A length scale for mixing through the cloud can be estimated from

$$X = \epsilon^{1/2} \tau^{3/2} \quad (1)$$

for a given energy dissipation rate,  $\epsilon$ , and a time scale for turbulent diffusion,  $\tau$ . The time from the SF<sub>6</sub> release to the point where the SF<sub>6</sub> had diffused through the cloud (pass 5) was 7.3 min. In the cloud the  $\epsilon$  values were about 125 cm<sup>2</sup> s<sup>-3</sup> during passes 1–5 (Fig. 8). Substituting these values in (1) gives  $X \sim 1$  km, or approximately the diameter of the cloud during passes 4 and 5.

Recent models for cloud mixing, such as Telford and Chai (1980), suggest that the newest regions of the cloud originate upshear, with downdrafts developing in the upper portions of older cloud parcels which have migrated downshear. They present evidence that the cycling of air up and down in a cloud is an essential mechanism by which cumulus clouds are diluted. This cycling is driven by mixing between fresh updrafts and downdrafts. The downdrafts originate from near cloud top due to the negative buoyancy produced by mixing of dry air into cloud top. Partial evaporation of the

smallest droplets in the downdraft, followed by mixing with the fresh droplets found in updrafts is responsible for producing the observed droplet spectra in cumuli. Entrainment of positive buoyancy into the downdraft and subsequent ascent drives the cycling process. This cycling continues until, after repeated mixing of the downdrafts with the updraft, enough of the air originating at cloud top has mixed downward to produce negative buoyancy throughout most of the cloud and the entire cloudy column collapses.

As suggested by the aforementioned model, the SF<sub>6</sub> plume on 19 July was carried up to cloud top levels on the upshear/upwind side (northwest) prior to complete mixing through the cloud. The downshear/downwind region was characterized by evaporating cloud, decreasing liquid water contents, colder temperatures, and downdrafts (Figs. 8 and 9).

Randall (1980) presents related criteria for conditional instability of the first kind upside-down (CIFKU). These are based on a two-layer model for a stratocumulus layer where an unsaturated parcel is entrained into the cloudy air below, cooled and moistened by evaporation, and accelerated downwind by the buoyancy force. The requirement for this instability is

$$\beta \Delta h - \epsilon' L \Delta(q + l) < 0, \quad (2)$$

where  $\epsilon' = C_p T / L$ ,  $h \equiv C_p T + gz + Lq$ ,  $\beta$  is a thermodynamic coefficient which is equal to 0.69 for the present case,  $L$  the latent heat of vaporization,  $C_p$  the specific heat at constant pressure,  $T$  the temperature,  $z$  the height of the parcel, and  $q$  and  $l$  the mixing ratios of vapor and liquid, respectively. The  $\Delta$  operator refers to the difference between the upper (dry) region and the lower-layer values. The cloud sampled on 19 July was more of an individual cumulus cloud (part of a scattered to broken layer) than a stratocumulus deck; the layer between 520 and 640 mb was only slightly stable (Fig. 6). However, if we apply (2) to the dry air above the cloud at 550 mb and the northwest region of the cloud during pass 1 or 2 (576 mb,  $T = -5^\circ\text{C}$ ), we find that condition (2) is satisfied. Had we used values for the lower cloud regions, the left-hand side of (2) would be even more negative. This suggests that CIFKU, or a negative buoyancy process as suggested by Telford and Chai, occurred on 19 July. However, a downdraft region is evident outside the cloud-top region in Fig. 8, pass 3, on the southeast side of the cloud turret. It is likely that this circulation affected the development of the downdraft in this turret in addition to the CIFKU mechanism in the cloud.

#### b. Ice production in a tagged AgI plume

On 18 July 1985, 0.057 kg km<sup>-1</sup> of SF<sub>6</sub> was released along with an AgI–AgCl smoke into a small stratocumulus cloud at a temperature of  $-8^\circ\text{C}$ . Because of the cloud's small size, it would normally not be considered a candidate for rain-increase cloud seeding. It was treated to study the properties of this seeding agent. A

single treatment pass of 3 min. was made between 1629 and 1632 MDT. The treatment pass was about 15 km long at the treatment aircraft's true air speed of 4.9 km min<sup>-1</sup>. The Citation, which was 400 m above the treatment aircraft at 5.5 km (MSL) sampled near the cloud top during treatment (pass 1, Fig. 10). This was followed by a second pass through the cloud tops (pass 2, Fig. 10). The cloud was only about 2.5 km across at this altitude, suggesting that most of the treatment pass was made out of the visible cloud. Cloud depth was estimated to be about 1 km at the time of treatment. Following pass 2 the visible cloud dissipated and a haze (which was due to ice crystals) was observed. At 1636 MDT the Citation descended to the treatment altitude and made a series of passes roughly perpendicular to the treatment line. Several indications of SF<sub>6</sub>, both with and without ice particles, were found. The Citation then climbed to 5.4 km to sample the upper regions of the plume at -10°C between 1707 and 1715 MDT. The results of the plume measurements are given in Fig. 10.

PMS 2DC images of the ice particles found in the plume are given in Fig. 11.

Except for pass 10 and 11, each of the ice crystal regions were collocated with regions of SF<sub>6</sub> (Fig. 10). Pass 10 and 11 had relatively high concentrations of ice and were just adjacent to high concentrations of SF<sub>6</sub>. Since, at this point, the plume had aged 25–28 min, ice particle fallout could have been responsible for separation of the SF<sub>6</sub> and ice crystals. Otherwise, no ice was found outside the SF<sub>6</sub> regions, suggesting that ice formation was limited to the seeding plume.

The first two ice regions (pass 3 and 4 in Fig. 10) contained relatively large (700 μm), possibly rimed, ice particles in relatively low (about one per liter) concentrations. These particles, the first to nucleate and grow, most likely formed just after treatment, before the liquid water in the cloud had dissipated. Accretional growth may have helped these grow larger than subsequent ice particles (Figs. 10 and 11). Since most of the regions sampled later did not form in the liquid water cloud, ice particle growth was probably limited to depositional growth. However, traces of liquid water below the minimum detectable by the JW (about 0.03 g m<sup>-3</sup>), might have been present for the initial activation of the agent by contact nucleation. If saturation with respect to water is assumed, only about 0.07 g m<sup>-3</sup> of water vapor would be available for particle growth, given the difference in water vapor partial pressures with respect to water and ice at the sampling pressure and temperature. The measured ice water contents (Fig. 10) in the passes were roughly equal to or less than this value, which suggests that the growth of the ice particles was most likely limited by the amount of water vapor present. This probably prevented many of the early ice particles from growing to detectable sizes. As diffusion of water vapor into these regions occurred, these particles could have grown to

detectable sizes. Consequently, the rate of ice particle production was limited both by the activation characteristics of the agent and by the mixing of moisture into the plume. Many regions of the plume were without ice particles; therefore, a substantial portion of the plume lacked sufficient moisture to nucleate and grow ice particles.

Even though this cloud was smaller than those treated with AgI seeding agent in the Marwitz and Stewart study, the number of ice particles produced as a function of time was similar (Fig. 12), excluding the SF<sub>6</sub> plume regions without ice particles.

Recent tests of the AgI agent in the Colorado State University cloud chamber indicated an ice crystal production effectiveness,  $E$ , of approximately  $2.5 \times 10^{13}$  and  $10^{15}$  ice crystals per gram of AgI at -8 and -12°C, respectively. Unlike the plume on 18 July, these tests were conducted in a supercooled 1.5 g m<sup>-3</sup> liquid water cloud which was maintained in the chamber. Consequently, this number represents an upper limit to the expected number of ice particles (per gram of AgI released) which could grow to detectable sizes on 18 July. We estimate the fraction,  $F$ , of nuclei activated and grown to detectable sizes by

$$F = \frac{Q_t C_i}{E Q_a C_t} \quad (3)$$

where  $Q_t$  and  $Q_a$  are the release rates of tracer and AgI, respectively, and  $C_i$  and  $C_t$  are the observed concentrations of ice and tracer, respectively. Using peak values for ice and tracer concentrations, a maximum  $F$  of 54% was observed 17.5 min after seeding (Fig. 13). The lower  $F$  values at 37 and 38 min after seeding result from the higher  $E$  value in (3), since these passes were made at -10°C rather than -8°C. The variations in  $F$  reflect the uneven activation and growth of the seeding agent, which is not surprising, since portions of the plume failed to produce any ice. Clearly, there was an abundance of ice nuclei in the treatment plume, which resulted in an overseeding condition.

#### 4. Summary

The clouds sampled on 18 and 19 July were too small to produce precipitation on the ground. However, as the two cases illustrate, they were good candidates to test the mixing and ice activation characteristics of AgI smokes in relatively simple cloud systems. Light weight, fast response analyzers are indispensable to these types of studies.

Each analyzer had some features which were particularly useful in our studies. The more elaborate flow control mechanism in the AV analyzer was helpful in reducing the effects of altitude on the instrument response, while the faster response and lower baseline noise level of the WSU analyzer were necessary to detect the small amounts of SF<sub>6</sub> which were present in many of the plumes. The differences between the two

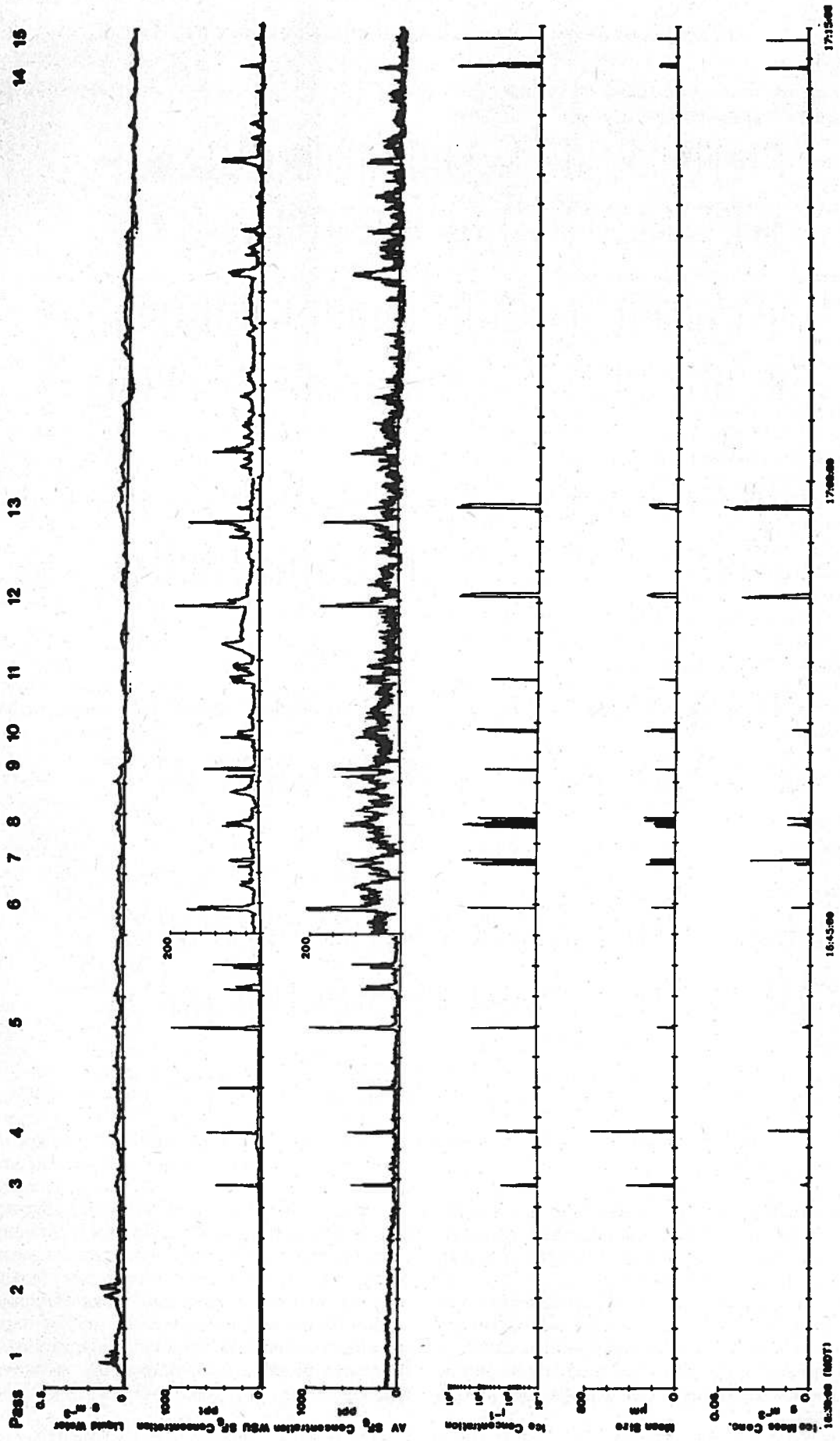


FIG. 10. The results of measurements made on 18 July 1985, from several passes through an AgI seeding plume which was released at 1631 MDT in a stratocumulus cloud. Ice particle concentrations are from the PMS 2DC probe. Volume mean size and ice mass concentration are computed assuming spherical particles of density  $0.3 \text{ g cm}^{-3}$ .

Pass

07/18/85 16:38:31.1701 16:38:35.



4

07/18/85 16:41:56.4388 16:41:57.



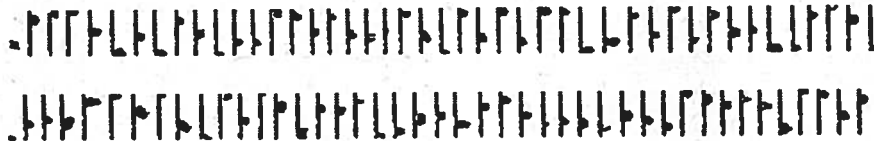
5

07/18/85 16:47:24.6547 16:47:25.



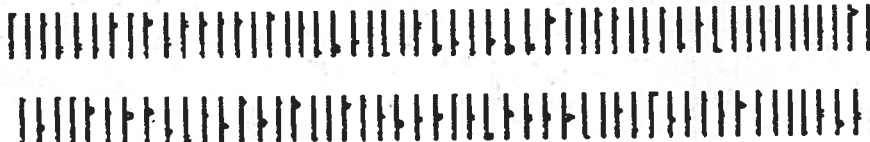
7

07/18/85 16:59:11.7489 16:59:12.



13

07/18/85 17:13:42.0503 17:13:42.



14

1mm

FIG. 11. PMS 2DC ice particle images for passes 4, 5, 7, 13 and 14 on 19 July 1985.

analyzers would have been less of a factor if more SF<sub>6</sub> had been released, however. Clearly, these analyzers can resolve cumulus-scale plume features from aircraft and document their evolution.

The tracer measurements on 19 July indicate a turbulent mixing zone, just below the cloud top, on the downwind/downshear side of the cumulus cloud. A CIFKU-type instability may have been present in this region. The mixing of the tracer through the cloud is

in accord with recent cumulus mixing theories, such as that of Telford and Chai. In our earlier studies of cumulus clouds, tracer releases into cloud-base updrafts during the early stages of cloud development resulted in comparatively narrow, more concentrated plumes at cloud midlevels. Further studies will be required to document the size and location of the mixing zone at different periods in the evolution of convective cloud systems.

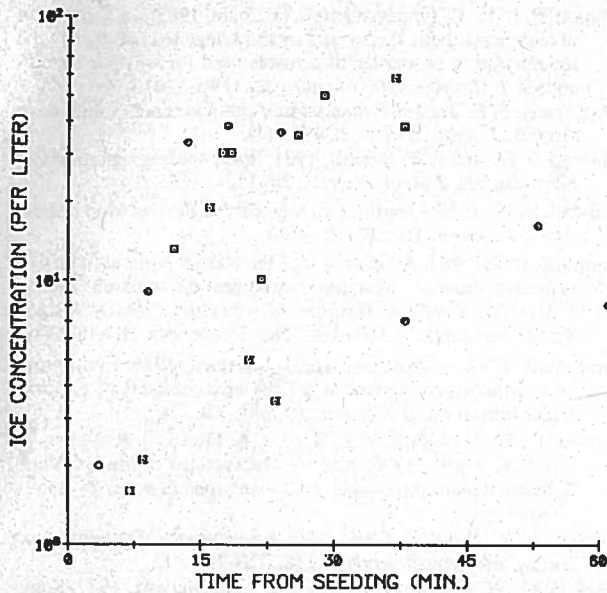


FIG. 12. Peak ice concentration in the seeding plume on 18 July 1985 (boxes) as a function of time from seeding. Results from Marwitz and Stewart (1981) are included (circles) for comparison.

For cloud mixing and dispersion studies in convective clouds, a variety of techniques should be possible with the  $SF_6$  tracer. One approach, as was done in the 19 July case, is to tag a cloudy air parcel (or cloud region) at a specific time and location with a single point or line release of  $SF_6$ . The advantage of this method is that it allows some history of the parcel movement in the cloud to be determined, as presented in section 3. A limitation to this technique is that it is difficult to follow the tagged parcel with an aircraft in convective clouds. Due to the relatively coarse resolution of the aircraft sampling passes and the rapid distortions of the  $SF_6$  plume, it is also difficult to adequately map the spatial distribution of the  $SF_6$ , especially in the early stages of the parcel evolution. However, when the parcel reaches a stable area (such as an anvil region) it should be much easier to obtain adequate cross sections of the plume, as these areas are likely to be more steady-state. By comparing the amounts of  $SF_6$  present in the anvil region from a single release at the base of a cumulonimbus cloud with the amount released, the fraction of cloud base air transported to the anvil could be determined.

A second technique would be to release large amounts of  $SF_6$  continuously, well upwind and below a cloud (or a developing cloud region), to produce a more homogeneous steady state  $SF_6$  concentration covering the base region of the cloud. Although this technique will not provide a history of an individual air parcel, it allows the dilution of cloud-base air to be measured directly as a function of height. Other techniques, such as releasing the  $SF_6$  outside of cloud (e.g., in a stable layer near the cloud top, or at cloud mid-

levels) should be useful to examine the entrainment process. Of course, proper targeting of the  $SF_6$  release may be difficult for the out-of-cloud release techniques. Future exploratory field investigations are planned to develop these various techniques.

Although candidates for AgI cloud seeding are generally larger than the 18 July cloud, it is reasonable to expect similar behavior in stable, slowly dispersing AgI plumes in clouds with low amounts of supercooled liquid water. Such clouds might be present in stable orographic situations, for example. As is clear from the 18 July case, the diffusion of water into the treatment plume is a major rate-controlling factor in these types of situations.

The 18 July measurements confirm that the tracer and seeding plumes remain colocated for relatively long periods of time, as the ice particles grow to detectable sizes. Even as the plumes separate (Fig. 10, passes 12 and 13) it is possible to associate the ice crystal plume with the  $SF_6$  plume, due to the similar width of the plumes and their close proximity.

The 18 July case also illustrates some of the uses for the  $SF_6$  tracer in the interpretation of seeding effects. It can be used to locate the portions of the seeding plume that were ineffective (i.e., that produce no measurable ice). For the rest of the seeding plume, the fraction of the total available seeding nuclei that have produced ice can also be estimated from (3). When natural ice is also present or suspected, (3) can also be used to estimate the maximum ( $F = 1$ ) contribution to the cloud ice concentration from the seeding agent (e.g., as in Stith et al., 1986).

The real time measurement capability of these analyzers allows several new  $SF_6$  tracer techniques to be

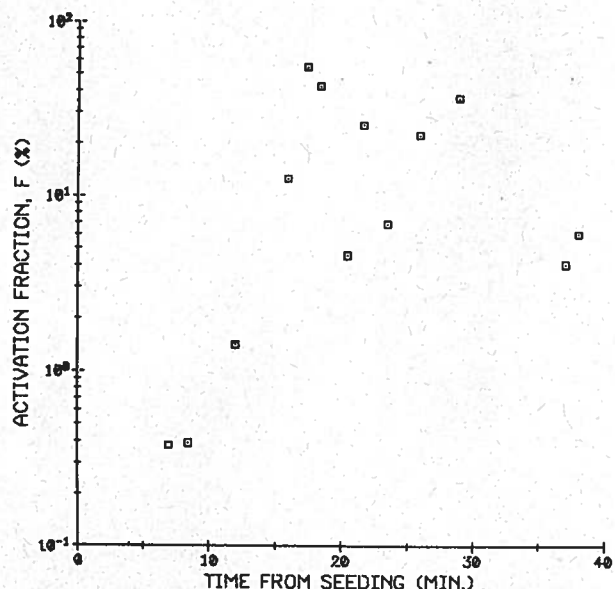


FIG. 13. Fraction of AgI ice nuclei activated as a function of time from seeding on 18 July 1985, based on (3).

used for in situ cloud studies. The SF<sub>6</sub> tracer technique can provide new information on the behavior of seeding plumes in clouds. This capability can now be directly applied in a variety of cloud seeding investigations. Much work remains to be done to fully develop and apply SF<sub>6</sub> tracer techniques to studies of cloud mixing and dispersion.

*Acknowledgments.* This work was supported by the National Oceanic and Atmospheric Administration, through the North Dakota State Weather Modification Board. Thanks are due to the members of the field crew, to Eloise Robertson for typing the manuscript, and especially to Mr. Don Griffith for his help in the analysis of the 18 July case study.

#### REFERENCES

- Baxter, R., D. Pankratz and I. Tombach, 1983: An advanced continuous SF<sub>6</sub> analyzer for real time tracer gas dispersion measurements from moving platforms. Paper No. CI 37, Presented at *Sixth World Conf. on Air Quality*, Paris.
- Benner, R. L., and B. Lamb, 1985: A fast response continuous analyzer for halogenated atmospheric tracers. *J. Atmos. Oceanic Technol.*, **2**, 582-589.
- Demott, P. J., W. G. Finnegan and L. O. Grant, 1983: An application of chemical kinetic theory and methodology to characterize the ice nucleating properties of aerosols used for weather modification. *J. Climate Appl. Meteor.*, **22**, 1190-1203.
- MacCready, P. B., Jr., 1964: Standardization of gustiness values from aircraft. *J. Appl. Meteor.*, **3**, 439-449.
- Marwitz, J. D., and R. E. Stewart, 1981: Some seeding signatures for Sierra storms. *J. Appl. Meteor.*, **20**, 1129-1144.
- Randall, D. A., 1980: Conditional instability of the first kind upside-down. *J. Atmos. Sci.*, **37**, 125-130.
- Reinking, R. F., 1985: An overview of the NOAA Federal-State Cooperative Program in weather modification research. *Fourth WMO Sci. Conf. on Weather Modification, WMO/IAMAD Symp.*, Honolulu, WMO/TD—No. 33, Geneva, II, 643-648.
- Simmonds, P. G., A. Lovelock and J. Lovelock, 1976: Continuous and ultrasensitive apparatus for the measurement of airborne tracer substances. *J. Chromatography*, **126**, 3-9.
- Stith, J. L., D. A. Griffith, R. L. Rose, J. A. Flueck, J. R. Miller, Jr. and P. L. Smith, 1986: Aircraft observations of transport and diffusion in cumulus clouds. *J. Climate Appl. Meteor.*, **25**, 1959-1970.
- Telford, J. W., and S. K. Chai, 1980: A new aspect of condensation theory. *Pure Appl. Geophys.* **118**, 720-742.
- Veal, D. L., W. A. Cooper, G. Vali and J. D. Marwitz, 1977: Some aspects of aircraft instrumentation for storm research. *Hail: Review of Hail Science and Hail Suppression, Meteor. Monogr.*, **16**, 237-255.